Journal of Materials Chemistry A

Evaluation of Brønsted Acidity and Proton Topology in Zr- and Hf-based Metal–Organic Frameworks Using Potentiometric Acid–Base Titration

Journal:	*Journal of Materials Chemistry A*
Manuscript ID	TA-ART-09-2015-007687.R1
Article Type:	Paper
Date Submitted by the Author:	23-Dec-2015
Complete List of Authors:	Klet, Rachel; Northwestern University, Chemistry Wang, Timothy; Northwestern Universtiy, Chemistry Liu, Yangyang; Northwestern University, Chemistry Hupp, J; Northwestern University, Department of Chemistry Farha, Omar; Northwestern University, Department of Chemistry

SCHOLARONE™
Manuscripts

Journal Name

ARTICLE

Evaluation of Brønsted Acidity and Proton Topology in Zr- and Hf-based Metal–Organic Frameworks Using Potentiometric Acid–Base Titration

Received 00th January 20xx,
Accepted 00th January 20xx

DOI: 10.1039/x0xx00000x

www.rsc.org/

Rachel C. Klet,[a] Yangyang Liu,[a] Timothy C. Wang,[a] Joseph T. Hupp[a,*] and Omar K. Farha[a,b,*]

Potentiometric acid–base titration is introduced as a method to evaluate pK_a values (Brønsted acidity) of protons present in the nodes of water stable Zr_6- and Hf_6-based metal–organic frameworks (MOFs), including UiO-type MOFs, NU-1000, and MOF-808. pK_a values were determined for the three typical types of protons present in these MOFs: μ_3–OH, M–OH_2, and M–OH (M = Zr, Hf). Additionally, the data was used to quantify defect sites resulting from either a surfeit or shortage of linkers in the MOFs and to provide information about the true proton topology of each material.

Introduction

Metal–organic frameworks (MOFs) are three-dimensionally structured porous materials composed of organic linkers and inorganic metal ions or clusters.[1-4] These materials possess rich tunable chemistry and have generated significant interest due to their potential applications for gas storage and separation,[5-8] sensing,[9, 10] and catalysis.[11-13] Zr- and Hf-based MOFs, in particular, are especially promising for practical applications due to their high water and chemical,[14-17] thermal,[18] and mechanical stability.[18, 19]

In considering these MOFs, one question that has not yet been well addressed is the Brønsted acidity of protons present on the inorganic nodes.[20] While this question is directly relevant to Brønsted acid-catalyzed reactions (and perhaps also for delineating the contributions of Lewis versus Brønsted acidity to catalysis),[21, 22] understanding the acidity of protons in the node may also help predict the outcomes of post-synthesis treatments such as Atomic Layer Deposition in MOFs (AIM),[23-26] or wet impregnation with reactive metal precursors.[26-32] Knowledge of Brønsted acidity may also prove instructive for understanding MOF proton conductivity.[33-36] One challenge to measuring the Brønsted acidity in MOFs is the lack of suitable/compatible characterization methods. For example, adsorption techniques commonly employed for inorganic solid acids, such as temperature-programmed desorption (TPD) with the probe molecules NH_3 or pyridine, are unlikely to be compatible with all but the most stable MOFs.[20, 37]

In order to both measure Brønsted acidity values and to better understand nuances in the proton topology of Zr- and Hf-based MOFs, we sought a method that would be: 1) accurate and reproducible, 2) quantitative, 3) technically easy to implement, and 4) compatible with a broad scope of MOFs. Potentiometric acid–base titrations have been employed to measure pK_a values of related porous materials including zirconium hydroxide.[38, 39] We felt that with appropriate considerations, this method could be extended to water-stable MOFs—the most important consideration being to ensure that the titrant has ample time to permeate the material fully and thereby interrogate all relevant interior sites. Acid–base titration has been used on a limited basis previously with MOFs, primarily to evaluate the labile proton content of materials functionalized with sulfonic acid groups.[40-43] Other authors (including us) have sought to gauge pK_a values, at least roughly, by measuring the pH values of MOF suspensions or coated disks.[21, 22, 44] But, we believe our current report to be the first comprehensive experimental study of MOF acid-base energetics as revealed by a systematic assessment of pK_as of polyprotic building units. As the focus of our study, we chose a series of hexa-Zr(IV)- and hexa-Hf(IV)-based MOFs. From the study, we conclude that, when coupled with other information, potentiometric titrations can yield not only information about local Brønsted acidity/basicity, but also insights into the identity and number of MOF defect sites, especially sites arising from either a surplus or a deficiency of linkers.

Results and Discussion

The MOF samples were prepared for potentiometric titration by dispersing in aqueous $NaNO_3$, then titrating with 0.1 M

[a] Department of Chemistry, Northwestern University, 2145 Sheridan Road, Evanston, IL 60208, United States. E-mail: j-hupp@northwestern.edu; o-farha@northwestern.edu
[b] Department of Chemistry, Faculty of Science, King Abdulaziz University, Jeddah, Saudi Arabia

Electronic Supplementary Information (ESI) available: Detailed experimental procedures and MOF characterization data, as well as additional figures and curve fittings. See DOI: 10.1039/x0xx00000x

This journal is © The Royal Society of Chemistry 20xx

Please do not adjust margins

aqueous HCl to adjust the pH to 3. The samples were then titrated with 0.1 M aqueous NaOH until the pH reached approximately 10.5. Titration curves were repeated for three samples of each material to gauge reproducibility.

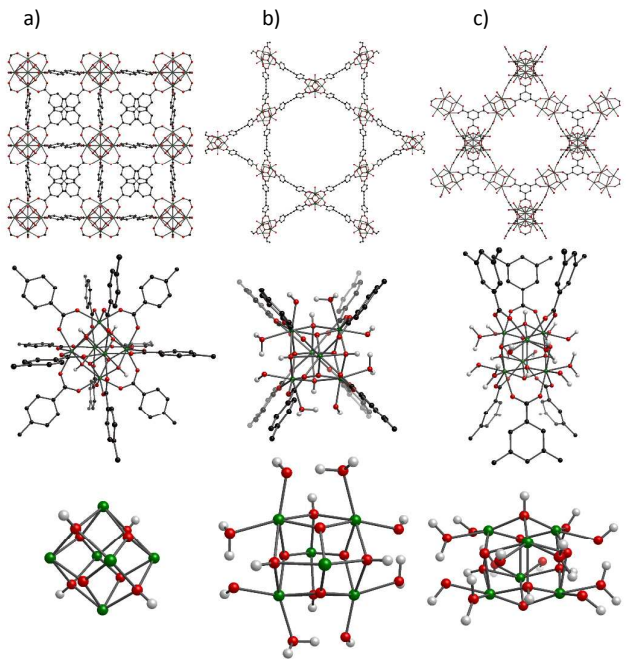

Fig. 1 M_6 nodes (M = Zr, Hf) showing 3D porous structure (top), node connectivity (middle), and proton topology (bottom) for (a) UiO-type MOFs (12-connected) (UiO-67 is shown on top), (b) NU-1000 (8-connected), and (c) MOF-808 (6-connected). Protons and carboxylate linkers have been omitted from the 3D porous and proton topology figures, respectively, for clarity. Zr/Hf, C, H, and O are shown in green, black, white, and red, respectively.

Titration of Zr-UiO-67 and Hf-UiO-67 (benzoic acid modulator). As starting points, we examined Zr-UiO-67 and Hf-UiO-67.[45] UiO-67, like its better-known congener, UiO-66, features a (nominally) 12-connected M_6 (M = Zr, Hf) cluster, $M_6(\mu_3\text{–}O)_4(\mu_3\text{–}OH)_4$ (Fig. 1a), with biphenyl-4,4'-dicarboxylate (BPDC) linkers. (See Electronic Supporting Information (ESI), Fig. S1b.) Assuming surface sites on MOF crystallites (which have unknown termination) can be largely ignored, and that negligibly few internal defects are present, then only one type of titratable proton—a M–μ_3–OH proton—is expected. Indeed, as shown in Figs. 2 and 3, for each MOF only one equivalence point is observed.[‡] The points are at pH = 7.1 ± 0.3 and pH = 7.7 ± 0.2 for Zr-UiO-67 and Hf-UiO-67, respectively, consistent with the assumption of nearly defect free compositions.[§] From the equivalence points, we calculate pK_a values for the M–μ_3–OH protons in Zr-UiO-67 of 3.44 ± 0.02 and in Hf-UiO-67 of 3.36 ± 0.01 (Table 1).[††] Overlays of titration curves from each of three samples of Zr-UiO-67 and of Hf-UiO-67 reveal excellent reproducibility (Fig. S27 and S28, ESI).

Titration of Zr-PCN-57 and Hf-PCN-57. We next investigated the Zr and Hf versions of PCN-57, an analogue of UiO-68.[18, 46] These materials have the typical 12-connected UiO-type cluster $M_6(\mu_3\text{–}O)_4(\mu_3\text{–}OH)_4$ (M = Zr, Hf) (Fig. 1a) and 2',3',5',6'-tetramethylterphenyl-4,4"-dicarboxylate (TPDC-4CH_3) linkers (Fig. S1c, ESI). Unfortunately, due to the highly hydrophobic nature of the TPDC-4CH_3 linker, as well as minimal missing-linker-related defects,[47] these samples do not disperse well in aqueous solution, complicating titration measurements. Nonetheless, while these data are not quantitative and should be interpreted with caution, they similarly show only one equivalence point, as indicated by one inflection point in each of the titration curve (at 5.4 and 6.0, respectively, for Zr-PCN-57 and Hf-PCN-57). For both materials, the corresponding pK_a value is 3.4 (Fig. 4, see ESI for first derivative curves, Fig. S29 and S30).[‡‡] This pK_a value is experimentally identical to those measured for Zr-UiO-67 (3.44 ± 0.02) and Hf-UiO-67 (3.36 ± 0.01) and we likewise assign it to the μ_3–OH protons (Table 1).

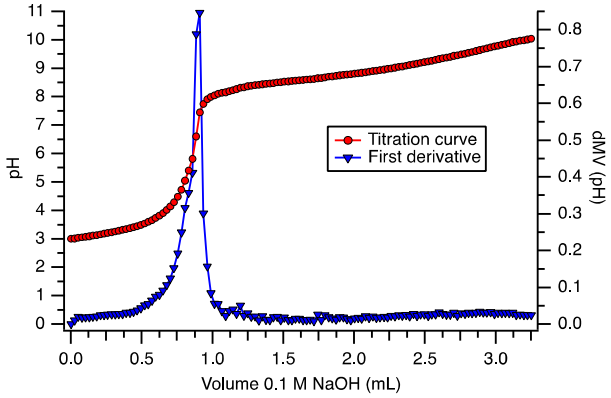

Fig 2 Acid–base titration curve of Zr-UiO-67 (red) and first derivative curve (blue).

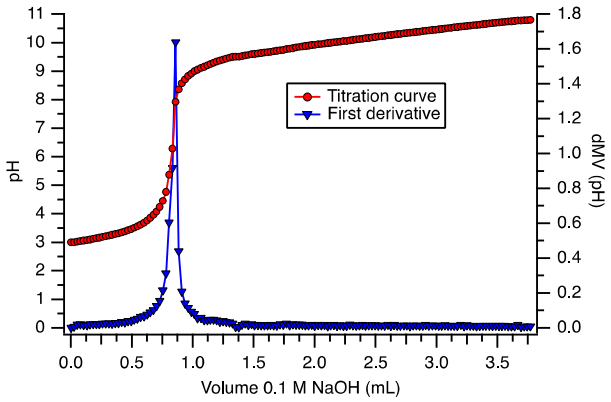

Fig. 3 Acid–base titration curve of Hf-UiO-67 (red) and first derivative curve (blue).

This journal is © The Royal Society of Chemistry 20xx

Please do not adjust margins

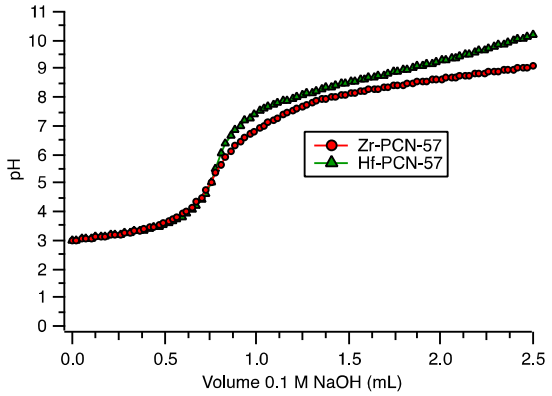

Fig. 4 Acid–base titration curves for Zr-PCN-57 (red) and Hf-PCN-57 (green).

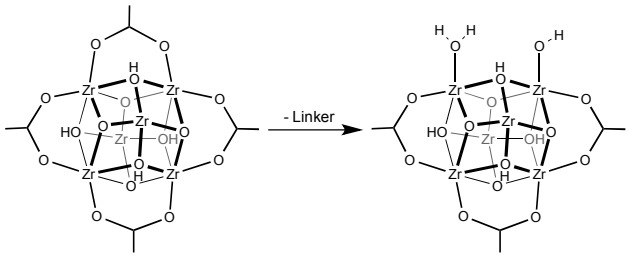

Fig. 5 Illustrative depiction of defect sites in UiO-66 from missing linkers. Some carboxylate linkers have been omitted for clarity.

Titration of Zr-UiO-66 and Hf-UiO-66. UiO-66 with terephthalate linkers (Fig. S1a, ESI) has been extensively studied and, compared to other UiO-type MOFs, defect sites arising from missing linkers are well documented.[19, 48-55] In fact, chemical catalysis by UiO-66 is often attributed to defect sites,[50, 52, 56-58] making their characterization and quantification of more than just structural interest. Although the exact identity of defect sites is unknown, most likely, missing linkers are replaced with $–OH_2$ and –OH groups in such a way as to compensate for the charge lost with the linkers (Fig. 5 and Fig. S14, ESI). (Depending on synthesis conditions, formate and/or chloride groups may also function as defect-sited charge-compensating ligands.) Estimates for missing linkers range as high as two per M_6 cluster,[51, 52] and the presence of any protons from defect sites should be evident by titration. Thus, for UiO-66 at least three types of protons are possible: μ_3–OH, $–OH_2$ and –OH protons. (The presence of defect sites in our samples of Zr-UiO-66 and Hf-UiO-66 are indicated by both N_2 sorption isotherms and thermogravimetric (TGA) analyses, see ESI). Acid–base titration of both Zr-UiO-66 and Hf-UiO-66 reveals curves with three apparent inflection points, which may correspond to these three types of protons (Fig. 6 and 7). To more accurately estimate the equivalence points in the titration curves, the first derivative curves were fit to Lorentzian-type peaks (Fig. S32 and S34, ESI). For Zr-UiO-66, the fits yielded equivalence points at 5.44 ± 0.04, 7.56 ± 0.01, and 9.51 ± 0.08, with corresponding pK_as of 3.52 ± 0.02, 6.79 ± 0.01, and 8.30 ± 0.02. Similarly, for Hf-UiO-66, equivalence points were measured at 5.3 ± 0.1, 7.25 ± 0.01, and 9.51 ± 0.07, with pK_as at 3.37 ± 0.02, 6.67 ± 0.03, and 8.14 ± 0.03 (Table 1). Based on similarity to pK_a values determined for UiO-67 and pK_{a1} for PCN-57, we assign the first pK_a value for each MOF (3.52 ± 0.02 and 3.37 ± 0.02 for Zr-UiO-66 and Hf-UiO-66, respectively) to the μ_3–OH proton. The other titratable protons then most likely correspond to defect sites in the node; we tentatively assign the second and third pK_a values to $M–OH_2$ and M–OH protons, respectively (Table 1).

Given the quantitative nature of titration, and assuming that each lost ditopic linker introduces one aqua and one hydroxo ligand at each of two nodes, it is tempting to try to determine the number of missing linkers in UiO-66 based on the number of titratable $M–OH_2$ protons and M–OH protons. The needed numbers can be calculated from the amount of NaOH titrant consumed between the first equivalence and last equivalence point. Using this method, we estimate 1.60 missing linkers for Zr-UiO-66 and 1.70 missing linkers for Hf-UiO-66 (of ideally 12 total; see Tables S3 and S5, ESI). These values seem reasonable based on literature reported values estimated by other methods; however, it should be noted that no consensus currently exists on the best method to quantify defect sites.[19, 50-52, 59] For comparison, using the TGA method of analyses for missing linkers, in which mass loss attributable to linker volatilization is compared to the expected value for the fully-connected MOF, we obtained missing linker values for Zr-UiO-66 and Hf-UiO-66 of 1.6 and 0.8, respectively (Fig. S15 and S16, Table S1, ESI); we believe the numbers obtained by titration are more representative of the true values, as potential TGA-related complications such as the presence of residual solvent and/or the thermolysis-based formation of nonvolatile carbonaceous byproducts are absent from the titration experiments. It is worth noting that defect site densities in UiO-66 are synthesis-protocol-dependent;[19] thus, the values reported here may well quantitatively describe only UiO-66 samples prepared by the same procedure.

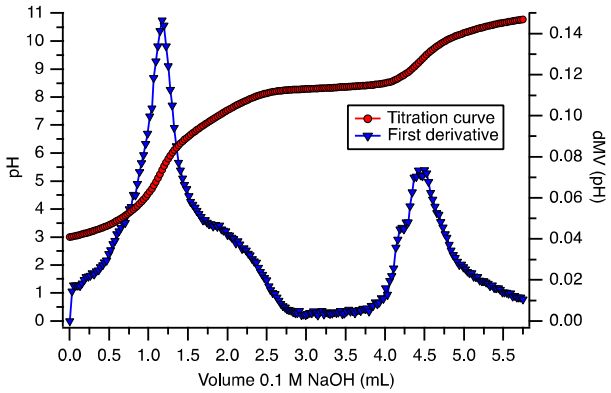

Fig. 6 Acid–base titration curve of Zr-UiO-66 (red) and first derivative curve (blue).

Please do not adjust margins

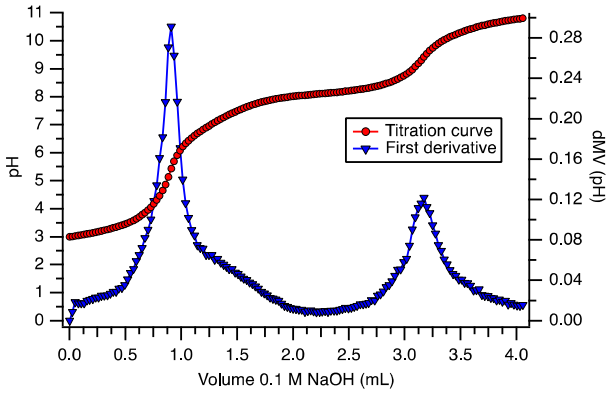

Fig. 7 Acid–base titration curve of Hf-UiO-66 (red) and first derivative curve (blue).

Titration of Zr-UiO-67 (hydrochloric acid modulator). Zr-UiO-67 has been reported as having no missing linker defects when synthesized with benzoic acid (*vide supra*)[54] or up to two missing linker defects when synthesized with instead hydrochloric acid or acetic acid as a growth modulator.[51, 59] Acid–base titration of a sample of Zr-UiO-67 synthesized using a method reported by us with hydrochloric acid as an additive yields a very complex titration curve, most likely indicative of missing-linker type defect sites, but perhaps also indicative of other types of defects (Fig. 8).[51,§§] While we found the titration curve difficult to model to determine equivalence points and calculate pK_a values (curve-fitting gave the best results with at least 4 peaks, see Fig. S38, ESI), we can calculate pK_a values that seem reasonable when compared to our data for related MOFs. For Zr-UiO-67(HCl), the pK_as were determined to be: 3.67 ± 0.01, 6.6 ± 0.2, 8.15 ± 0.02, and 9.14 ± 0.01 (Table 1). The first three pK_a values are similar to those measured in Zr-UiO-66 and Hf-UiO-66, corresponding to our assignments of μ_3–OH, Zr–OH_2, and Zr–OH. The fourth pK_a value is tentatively ascribed to deprotonation of a MOF decomposition product. It is worth noting that post-experiment PXRD assessment of material titrated to pH = 9 (below the unexpected fourth equivalence point at 9.9 ± 0.03) shows that, even though the sample has not dissolved, its crystallinity has been lost. Notably, Zr-UiO-67(HCl) is less stable toward basic solutions than other MOFs examined. These MOFs, whose titrations do not yield a fourth equivalence point, generally lose crystallinity only at pH values >9.

We did attempt to determine the number of missing linkers in Zr-UiO-67(HCl) using the same method employed for Zr-UiO-66 and Hf-UiO-66. Based on the amount of titrant consumed between the first and last apparent equivalence points, we estimate that Zr-UiO-67(HCl) is missing ~1.65 of an ideal 12 linkers, *i.e.* similar to the value measured for UiO-66.[||] (Again for comparison, by using TGA, we obtained a value of 1.3 missing linkers, Fig. S17 and Table S1, ESI). While the cause of the greater titration complexity for Zr-UiO-67(HCl) compared to UiO-66 is unknown, one can speculate that it may be related to a low-symmetry distribution of defects within Zr-UiO-67(HCl) resulting in different pK_a values for similar-type protons (μ_3–OH, M–OH_2, M–OH) in different environments. (Examples of differing environments might be nodes featuring one vs. two vs. three missing linkers, or pairs of linker loss sites arranged proximal to vs. far from each other on a given node.) Notably, Goodwin *et al.* suggest that defect siting in Hf-UiO-66 is significantly correlated, i.e. spatial distributions of defects are not random; no such study has been reported for UiO-67.[53]

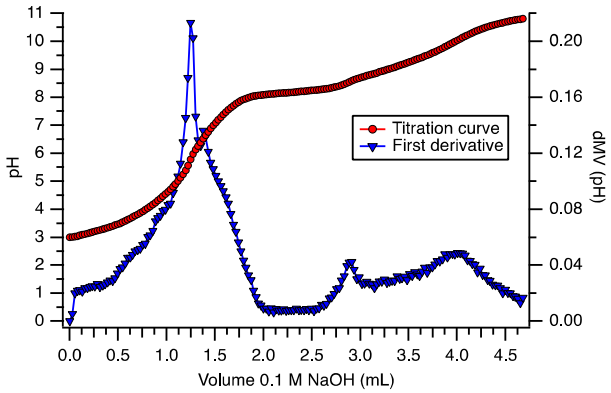

Fig. 8 Acid–base titration curve of Zr-UiO-67(HCl) (red) and first derivative curve (blue).

Titration of NU-1000. We next turned our attention to the 8-connected Zr_6 MOF, NU-1000.[26] This material contains a tetratopic carboxylate linker 1,3,6,8-tetrakis(*p*-benzoate)pyrene (TBAPy) (Fig. S1d, ESI) and $Zr_6(\mu_3–O)_4(\mu_3–OH)_4(OH)_4(H_2O)_4$ nodes—the detailed proton topology of which has recently been reported by us based on combined experimental spectroscopic and computational analyses (Fig. 1b).[60] Based on the assigned node topology, we anticipated at least three types of protons to be indicated by titration, similar to defective UiO-66. Acid–base titration of NU-1000 yields curves with at least two equivalence points (Fig. 9). When the first derivative of the titration curve is fit to Lorentzian-type peaks (Fig. S36, ESI), three pK_a values are obtained: 3.59 ± 0.02, 5.75 ± 0.04, 8.2 ± 0.1 (Table 1). Notably, these values are similar to those obtained for UiO-66, and like UiO-66, we assign to μ_3–OH protons, Zr–OH_2 protons, and Zr–OH protons, respectively.

In our first report of NU-1000, we noted that a fully 12-connected secondary framework could be located crystallographically with an occupancy of ~20%. Modeling this secondary framework as $[Zr_6(\mu_3–O)_4(\mu_3–OH)_4]_2(TBAPy)_6$ clusters in the mesopores of NU-1000 at an occupancy of 25% led to a simulated N_2 adsorption isotherm that is in excellent agreement with the experimental isotherm.[26] We can potentially quantify the number of defects (resulting from a surplus of linkers) according to the acid–base titration curve for NU-1000. If we consider the total amount of titrant (0.1 M NaOH) consumed for an approximately 50 mg sample of NU-1000, we find that only ca. 61% of the expected moles of OH^- (for a defect-free material) has been consumed. If we then assume that extra linkers and nodes occupy the framework at approximately 25% (resulting in replacement of Zr–OH_2 and Zr–OH protons with surplus linkers and noting additional μ_3–OH protons with extra nodes), then, pleasingly, we find

This journal is © The Royal Society of Chemistry 20xx

Please do not adjust margins

excellent agreement (*ca.* 97%) between the moles OH^- consumed and the expected value (Table S7, ESI). It should be noted, however, that further quantification of moles OH^- consumed by each type of proton (μ_3–OH, Zr–OH_2, or Zr–OH) breaks down—most likely due to difficulty in separating deprotonation steps, as evidenced by the lack of separation between inflection points (or equivalence points) in the titration curve. Nonetheless, these results point to the value of potentiometric acid–base titrations for quantifying defect sites in Zr- and Hf-based MOFs resulting from either a surfeit or deficiency of linkers.

Titration of MOF-808. MOF-808 is a 6-connected MOF featuring $Zr_6(\mu_3\text{–}O)_4(\mu_3\text{–}OH)_4(HCOO)_6$ clusters and benzene-1,3,5-tricarboxylate (BTC) linkers (Fig. S1e, ESI).[14, 16] Upon thermal activation in fresh solvent, the formate ions are presumably replaced with –OH_2 and –OH ligands to yield $Zr_6(\mu_3\text{–}O)_4(\mu_3\text{–}OH)_4(OH)_6(OH_2)_6$ nodes (Fig. 1c).[61] Thus, in terms of titratable protons, activated MOF-808 is anticipated to be similar to defective UiO-66 or NU-1000 with three types of protons corresponding to μ_3–OH, –OH_2, and –OH protons. Acid–base titration of activated MOF-808, however, reveals four distinct equivalence points at 5.14 ± 0.07, 7.55 ± 0.06, 8.74 ± 0.02, and 10.02 ± 0.03 (Fig. 10), resulting in pK_a values at 3.64 ± 0.01, 6.22 ± 0.04, 8.23 ± 0.04, and 9.12 ± 0.02, respectively (Table 1). Similar to Zr-UiO-67(HCl), with MOF-808 we observe three pK_a values that appear representative of MOFs with M_6-based (M = Zr, Hf) nodes with μ_3–OH, M–OH_2, and M–OH protons, as well as a fourth pK_a value at higher pH which is as yet unassigned.††† These results may nonetheless indicate that MOF-808 has a more complex proton topology than suggested by the molecular formula. It is also worth noting that the total moles of titrant consumed for samples of MOF-808 corresponds to only ca. 68% of the moles of OH^- expected based on the assigned crystal structure and node composition. Whether the discrepancy is indicative of a more complex than proposed node proton distribution, an excess of linkers beyond those defining the solved single-crystal X-ray structure, or some other factor is unclear. Variable-temperature diffuse-reflectance infrared Fourier transform spectroscopy (DRIFTS) measurements, like those recently reported for NU-1000 might prove enlightening.‡‡‡

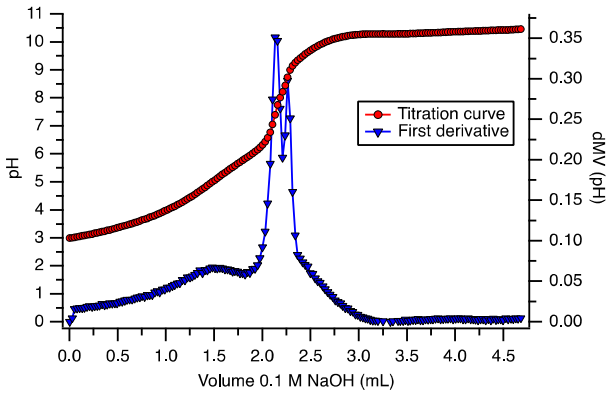

Fig. 9 Acid–base titration curve of NU-1000 (red) and first derivative curve (blue).

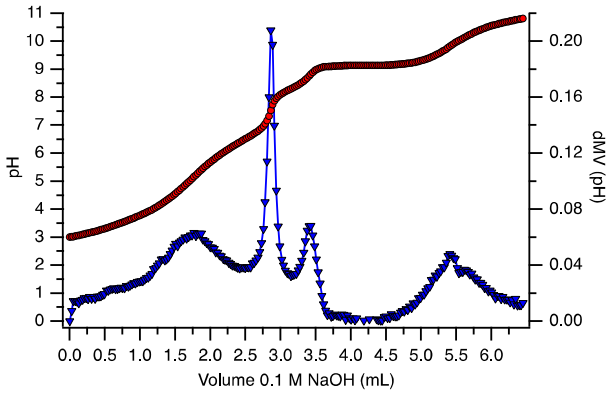

Fig. 10 Acid–base titration curve of MOF-808 (red) and first derivative curve (blue).

Table 1 Calculated pK_a values for UiO-66, UiO-67, PCN-57, NU-1000, and MOF-808

MOF	pK_{a1} μ_3-OH	pK_{a2} –OH_2	pK_{a3} –OH
Zr-UiO-67	3.44 ± 0.02	–	–
Hf-UiO-67	3.36 ± 0.01	–	–
Zr-PCN-57	~3.4	–	–
Hf-PCN-57	~3.4	–	–
Zr-UiO-66	3.52 ± 0.02	6.79 ± 0.01	8.30 ± 0.02
Hf-UiO-66	3.37 ± 0.02	6.67 ± 0.03	8.14 ± 0.03
Zr-UiO-67(HCl)	3.67 ± 0.01	6.6 ± 0.2	8.15 ± 0.02
NU-1000	3.59 ± 0.02	5.75 ± 0.04	8.2 ± 0.1
MOF-808	3.64 ± 0.01	6.22 ± 0.04	8.23 ± 0.04

Experimental Section

Potentiometric titrations were completed with a Metrohm Titrando 905 equipped with Dosino 800 20-mL and 10-mL dosing units using procedures similar to those reported for $Zr(OH)_4$.[38, 39] Calibration was performed with commercial pH buffers 2.00, 4.00, 7.00, and 9.00 (Metrohm). Prior to titration, MOF samples were ground with a mortar and pestle, and then approximately 50 mg of sample was dispersed in approximately 60 mL of 0.01 M aq. $NaNO_3$ solution, covered with parafilm, and allowed to equilibrate for 18 h. Each titration solution was charged with a magnetic stir bar, adjusted using 0.1 M aq. HCl to a pH of 3, and then titrated with 0.1 M aq. NaOH to a pH of 10.5–11 using injection volumes of 0.025 mL and an injection rate of 0.02 mL/min. Titration curves were collected for three samples of each MOF. Equivalence points were obtained from the first derivative of the resulting titration curve of pH as a function of volume of titrant added, where the maximum points in the derivative curve correspond to inflection points and indicate equivalence points. pK_a values were determined as the pH at one-half of the volume of titrant added to reach the equivalence point. When more than one peak was observed in the first derivative curve, the data were subjected to curve-fitting using IGOR Pro 6.36 (WaveMetrics, Inc.) with Lorentzian functions.

Conclusions

Potentiometric acid–base titration is an effective experimental technique for determining Brønsted acidities of node protons in water stable Zr- and Hf-based MOFs. Using this technique, pK_a values have been assigned to the μ_3–OH, –OH_2, or –OH protons common to these MOFs. A fourth pK_a value, indicating a fourth type of proton (whose chemical identity has not yet been determined), was observed for both Zr-UiO-67(HCl) and MOF-808; computational studies may prove useful for elucidating the proton topologies in these complex materials. Titrations are also useful for quantifying defect sites resulting from either a surfeit (NU-1000) or deficit (UiO's) of linkers. As water-stable MOFs move toward the fore, and as the potential significance of defect sites in defining MOF functional chemistry is increasingly appreciated, we believe that potentiometric acid-base titration will prove to be of considerable unique, as well as complementary, value for characterizing these ubiquitous compounds.

Acknowledgments

This work was supported, in part, by the Nanoporous Materials Genome Center, funded by the U.S. DOE, Office of Science, Basic Energy Sciences Program (Award DE-FG02-12ER16362) and by Northwestern University This work made use of the J. B. Cohen X-Ray Diffraction Facility supported by the MRSEC program of the National Science Foundation (DMR-1121262) at the Materials Research Center of Northwestern University. We thank Dr. D. A. Gómez-Gualdrón for computational assistance with the proposed crystal structure for MOF-808.

Notes and references

‡Our speculative explanation for the observation of only one equivalence point (rather than multiple equivalence points as is typically observed for a weak polyprotic acid) is that the four structurally equivalent μ_3–OH protons are separated by a total of 24 highly ionic Zr(IV)–oxygen(carboxylate) bonds. We further speculate that the sodium ions that replace the titrated protons are ion-paired to the MOF nodes, providing yet more screening.

§The small shoulder to the left of the main peak in the first derivative curve for Zr-UiO-67 (Fig. 2) may be indicative of some missing linkers, especially compared to Hf-UiO-67 (Fig. 3), which appears to be entirely defect-free.

††pK_a values are independent of concentration (but not independent of temperature, ionic strength, and solvent dielectric constant), while equivalence points are dependent on concentration. Thus, the larger standard deviation on the equivalence point value compared to the pK_a value may reflect small differences in concentration between runs.

‡‡Due to the difficulty in dispersing these materials in aqueous solution, multiple trials were not attempted.

§§Defective Zr-UiO-67(HCl) samples disperse noticeably better in aqueous solution than the apparently non-defective Zr-UiO-67 samples synthesized with benzoic acid, in accord with the expected increase in hydrophilicity for defective samples. See ref. 32.

||If the last apparent equivalence point for Zr-UiO-67(HCl) is due to titration of a site introduced by MOF degradation, the value for the number of missing linkers could be as low as 1.10.

†††Post-experiment PXRD assessment of a sample of MOF-808 titrated to pH = 10 indicated that crystallinity had been lost. Accordingly, the unexpected fourth equivalence point at 10.02 ± 0.03 may correspond to deprotonation of a decomposition product of the MOF (*i.e.*, a structurally ill-defined coordination polymer); however, no such peak was observed upon decomposition of other MOFs at high pH values putting this assignment in question.

‡‡‡This result might also suggest incomplete activation of MOF-808.

1. O. M. Yaghi, M. O'Keeffe, N. W. Ockwig, H. K. Chae, M. Eddaoudi and J. Kim, *Nature*, 2003, **423**, 705-714.
2. S. Horike, S. Shimomura and S. Kitagawa, *Nat Chem*, 2009, **1**, 695-704.
3. G. Ferey, *Chem. Soc. Rev.*, 2008, **37**, 191-214.
4. O. K. Farha and J. T. Hupp, *Acc. Chem. Res.*, 2010, **43**, 1166-1175.
5. M. Dincă and J. R. Long, *Angew. Chem. Int. Ed.*, 2008, **47**, 6766-6779.
6. J.-R. Li, R. J. Kuppler and H.-C. Zhou, *Chem. Soc. Rev.*, 2009, **38**, 1477-1504.
7. O. K. Farha, A. Özgür Yazaydın, I. Eryazici, C. D. Malliakas, B. G. Hauser, M. G. Kanatzidis, S. T. Nguyen, R. Q. Snurr and J. T. Hupp, *Nat. Chem.*, 2010, **2**, 944-948.
8. H. Furukawa, N. Ko, Y. B. Go, N. Aratani, S. B. Choi, E. Choi, A. Ö. Yazaydin, R. Q. Snurr, M. O'Keeffe, J. Kim and O. M. Yaghi, *Science*, 2010, **329**, 424-428.
9. L. E. Kreno, K. Leong, O. K. Farha, M. Allendorf, R. P. Van Duyne and J. T. Hupp, *Chem. Rev.*, 2012, **112**, 1105-1125.
10. Z. Hu, B. J. Deibert and J. Li, *Chem. Soc. Rev.*, 2014, **43**, 5815-5840.
11. D. Farrusseng, S. Aguado and C. Pinel, *Angew. Chem. Int. Ed.*, 2009, **48**, 7502-7513.
12. J. Lee, O. K. Farha, J. Roberts, K. A. Scheidt, S. T. Nguyen and J. T. Hupp, *Chem. Soc. Rev.*, 2009, **38**, 1450-1459.
13. M. Yoon, R. Srirambalaji and K. Kim, *Chem. Rev.*, 2012, **112**, 1196-1231.
14. H. Furukawa, F. Gándara, Y.-B. Zhang, J. Jiang, W. L. Queen, M. R. Hudson and O. M. Yaghi, *J. Am. Chem. Soc.*, 2014, **136**, 4369-4381.
15. H.-L. Jiang, D. Feng, K. Wang, Z.-Y. Gu, Z. Wei, Y.-P. Chen and H.-C. Zhou, *J. Am. Chem. Soc.*, 2013, **135**, 13934-13938.
16. W. Liang, H. Chevreau, F. Ragon, P. D. Southon, V. K. Peterson and D. M. D'Alessandro, *CrystEngComm*, 2014, **16**, 6530-6533.
17. J. E. Mondloch, M. J. Katz, N. Planas, D. Semrouni, L. Gagliardi, J. T. Hupp and O. K. Farha, *Chem. Commun.*, 2014, **50**, 8944-8946.
18. J. H. Cavka, S. Jakobsen, U. Olsbye, N. Guillou, C. Lamberti, S. Bordiga and K. P. Lillerud, *J. Am. Chem. Soc.*, 2008, **130**, 13850-13851.
19. H. Wu, Y. S. Chua, V. Krungleviciute, M. Tyagi, P. Chen, T. Yildirim and W. Zhou, *J. Am. Chem. Soc.*, 2013, **135**, 10525-10532.
20. J. Jiang and O. M. Yaghi, *Chem. Rev.*, 2015, **115**, 6966-6997.
21. A. Herbst, A. Khutia and C. Janiak, *Inorg. Chem.*, 2014, **53**, 7319-7333.
22. Y.-X. Zhou, Y.-Z. Chen, Y. Hu, G. Huang, S.-H. Yu and H.-L. Jiang, *Chem. Eur. J.*, 2014, **20**, 14976-14980.

This journal is © The Royal Society of Chemistry 20xx

Please do not adjust margins

23. C.-W. Kung, J. E. Mondloch, T. C. Wang, W. Bury, W. Hoffeditz, B. M. Klahr, R. C. Klet, M. J. Pellin, O. K. Farha and J. T. Hupp, *ACS Appl. Mater. Interfaces*, 2015, DOI: 10.1021/acsami.5b06901.
24. I. S. Kim, J. Borycz, A. E. Platero-Prats, S. Tussupbayev, T. C. Wang, O. K. Farha, J. T. Hupp, L. Gagliardi, K. W. Chapman, C. J. Cramer and A. B. F. Martinson, *Chem. Mater.*, 2015, **27**, 4772-4778.
25. A. W. Peters, Z. Li, O. K. Farha and J. T. Hupp, *ACS Nano*, 2015, **9**, 8484-8490.
26. J. E. Mondloch, W. Bury, D. Fairen-Jimenez, S. Kwon, E. J. DeMarco, M. H. Weston, A. A. Sarjeant, S. T. Nguyen, P. C. Stair, R. Q. Snurr, O. K. Farha and J. T. Hupp, *J. Am. Chem. Soc.*, 2013, **135**, 10294-10297.
27. R. C. Klet, S. Tussupbayev, J. Borycz, J. R. Gallagher, M. M. Stalzer, J. T. Miller, L. Gagliardi, J. T. Hupp, T. J. Marks, C. J. Cramer, M. Delferro and O. K. Farha, *J. Am. Chem. Soc.*, 2015, DOI: 10.1021/jacs.5b11350.
28. O. V. Gutov, M. G. Hevia, E. C. Escudero-Adán and A. Shafir, *Inorg. Chem.*, 2015, **54**, 8396-8400.
29. S. Yuan, Y.-P. Chen, J. Qin, W. Lu, X. Wang, Q. Zhang, M. Bosch, T.-F. Liu, X. Lian and H.-C. Zhou, *Angew. Chem. Int. Ed.*, 2015, **54**, 14696-14700.
30. D. Yang, S. O. Odoh, T. C. Wang, O. K. Farha, J. T. Hupp, C. J. Cramer, L. Gagliardi and B. C. Gates, *J. Am. Chem. Soc.*, 2015, **137**, 7391-7396.
31. H. G. T. Nguyen, N. M. Schweitzer, C.-Y. Chang, T. L. Drake, M. C. So, P. C. Stair, O. K. Farha, J. T. Hupp and S. T. Nguyen, *ACS Catalysis*, 2014, **4**, 2496-2500.
32. C. Larabi and E. A. Quadrelli, *Eur. J. Inorg. Chem.*, 2012, **2012**, 3014-3022.
33. N. C. Jeong, B. Samanta, C. Y. Lee, O. K. Farha and J. T. Hupp, *J. Am. Chem. Soc.*, 2012, **134**, 51-54.
34. S. Horike, D. Umeyama and S. Kitagawa, *Acc. Chem. Res.*, 2013, **46**, 2376-2384.
35. M. Yoon, K. Suh, S. Natarajan and K. Kim, *Angew. Chem. Int. Ed.*, 2013, **52**, 2688-2700.
36. J. J. Gassensmith, J. Y. Kim, J. M. Holcroft, O. K. Farha, J. F. Stoddart, J. T. Hupp and N. C. Jeong, *J. Am. Chem. Soc.*, 2014, **136**, 8277-8282.
37. W. Morris, C. J. Doonan and O. M. Yaghi, *Inorg. Chem.*, 2011, **50**, 6853-6855.
38. T. J. Bandosz, M. Laskoski, J. Mahle, G. Mogilevsky, G. W. Peterson, J. A. Rossin and G. W. Wagner, *J. Phys. Chem. C*, 2012, **116**, 11606-11614.
39. T. G. Glover, G. W. Peterson, J. B. DeCoste and M. A. Browe, *Langmuir*, 2012, **28**, 10478-10487.
40. C.-Y. Sun, S.-X. Liu, D.-D. Liang, K.-Z. Shao, Y.-H. Ren and Z.-M. Su, *J. Am. Chem. Soc.*, 2009, **131**, 1883-1888.
41. G. Akiyama, R. Matsuda, H. Sato, M. Takata and S. Kitagawa, *Adv. Mater.*, 2011, **23**, 3294-3297.
42. J. Juan-Alcaniz, R. Gielisse, A. B. Lago, E. V. Ramos-Fernandez, P. Serra-Crespo, T. Devic, N. Guillou, C. Serre, F. Kapteijn and J. Gascon, *Catal. Sci. Technol.*, 2013, **3**, 2311-2318.
43. J. Chen, K. Li, L. Chen, R. Liu, X. Huang and D. Ye, *Green Chem.*, 2014, **16**, 2490-2499.
44. M. H. Beyzavi, R. C. Klet, S. Tussupbayev, J. Borycz, N. A. Vermeulen, C. J. Cramer, J. F. Stoddart, J. T. Hupp and O. K. Farha, *J. Am. Chem. Soc.*, 2014, **136**, 15861-15864.
45. P. Xydias, I. Spanopoulos, E. Klontzas, G. E. Froudakis and P. N. Trikalitis, *Inorg. Chem.*, 2014, **53**, 679-681.
46. H.-L. Jiang, D. Feng, T.-F. Liu, J.-R. Li and H.-C. Zhou, *J. Am. Chem. Soc.*, 2012, **134**, 14690-14693.
47. P. Ghosh, Y. J. Colon and R. Q. Snurr, *Chem. Commun.*, 2014, **50**, 11329-11331.
48. L. Valenzano, B. Civalleri, S. Chavan, S. Bordiga, M. H. Nilsen, S. Jakobsen, K. P. Lillerud and C. Lamberti, *Chem. Mater.*, 2011, **23**, 1700-1718.
49. S. Jakobsen, D. Gianolio, D. S. Wragg, M. H. Nilsen, H. Emerich, S. Bordiga, C. Lamberti, U. Olsbye, M. Tilset and K. P. Lillerud, *Phys. Rev. B*, 2012, **86**, 125429.
50. F. Vermoortele, M. Vandichel, B. Van de Voorde, R. Ameloot, M. Waroquier, V. Van Speybroeck and D. E. De Vos, *Angew. Chem. Int. Ed.*, 2012, **51**, 4887-4890.
51. M. J. Katz, Z. J. Brown, Y. J. Colon, P. W. Siu, K. A. Scheidt, R. Q. Snurr, J. T. Hupp and O. K. Farha, *Chem. Commun.*, 2013, **49**, 9449-9451.
52. F. Vermoortele, B. Bueken, G. Le Bars, B. Van de Voorde, M. Vandichel, K. Houthoofd, A. Vimont, M. Daturi, M. Waroquier, V. Van Speybroeck, C. Kirschhock and D. E. De Vos, *J. Am. Chem. Soc.*, 2013, **135**, 11465-11468.
53. M. J. Cliffe, W. Wan, X. Zou, P. A. Chater, A. K. Kleppe, M. G. Tucker, H. Wilhelm, N. P. Funnell, F.-X. Coudert and A. L. Goodwin, *Nat. Commun.*, 2014, **5**.
54. S. Øien, D. Wragg, H. Reinsch, S. Svelle, S. Bordiga, C. Lamberti and K. P. Lillerud, *Cryst. Growth Des.*, 2014, **14**, 5370-5372.
55. Z. Fang, B. Bueken, D. E. De Vos and R. A. Fischer, *Angew. Chem. Int. Ed.*, 2015, DOI: 10.1002/anie.201411540.
56. F. Vermoortele, R. Ameloot, A. Vimont, C. Serre and D. De Vos, *Chem. Commun.*, 2011, **47**, 1521-1523.
57. M. J. Katz, J. E. Mondloch, R. K. Totten, J. K. Park, S. T. Nguyen, O. K. Farha and J. T. Hupp, *Angew. Chem. Int. Ed.*, 2014, **53**, 497-501.
58. J. E. Mondloch, M. J. Katz, W. C. Isley III, P. Ghosh, P. Liao, W. Bury, G. W. Wagner, M. G. Hall, J. B. DeCoste, G. W. Peterson, R. Q. Snurr, C. J. Cramer, J. T. Hupp and O. K. Farha, *Nat. Mater.*, 2015, **14**, 512-516.
59. G. C. Shearer, S. Forselv, S. Chavan, S. Bordiga, K. Mathisen, M. Bjørgen, S. Svelle and K. P. Lillerud, *Top. Catal.*, 2013, **56**, 770-782.
60. N. Planas, J. E. Mondloch, S. Tussupbayev, J. Borycz, L. Gagliardi, J. T. Hupp, O. K. Farha and C. J. Cramer, *J. Phys. Chem. Lett.*, 2014, **5**, 3716-3723.
61. S.-Y. Moon, Y. Liu, J. T. Hupp and O. K. Farha, *Angew. Chem. Int. Ed.*, 2015, **54**, 6795-6799.

1

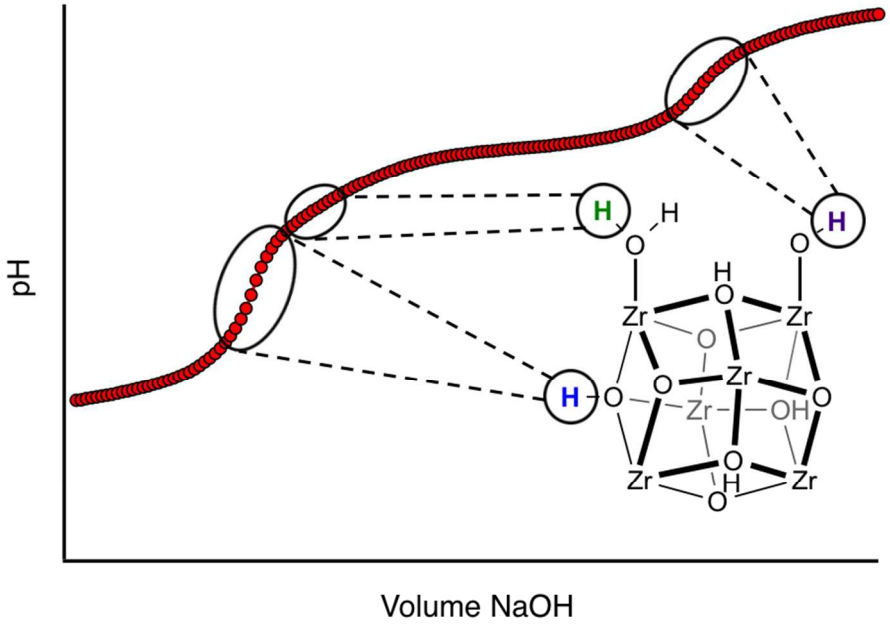
pH
Volume NaOH
H
H
H
O
O
H
O
Zr
Zr
O
Zr
O
O
Zr
OH
O
Zr
O
H
Zr
O